Laplacian growth phenomena with the third boundary condition: Crossover from dense structure to diffusion-limited aggregation fractal

Takashi Nagatani College of Engineering, Shizuoka University, Hamamatsu 432, Japan (Received 17 July 1989)

A Laplacian growth model with the third boundary condition, $(1-P)\partial\Phi/\partial n - P\Phi = 0$, is considered in order to study the effect of the sticking probability of the diffusion-limited aggregation (DLA), where Φ is the harmonic function satisfying the Laplace equation and $\partial \Phi / \partial n$ the derivative normal to the interface. The crossover from the dense structure to the DLA fractal is investigated by using a two-parameter position-space renormalization-group method. A global flow diagram in two-parameter space is obtained. It is found that there are two nontrivial fixed points, the Eden point and the DLA point. The DLA point corresponding to the DLA fractal is stable in all directions, while the Eden point is a saddle point. When the sticking probability P is not 1, the aggregate must eventually cross over to the DLA fractal. The crossover exponent ϕ and crossover radius r_{\times} are calculated.

I. INTRODUCTION

Fractal growth phenomena in pattern formation¹⁻¹¹ have recently attracted considerable attention. Examples of pattern formation in diffusive systems include viscous fingering, electrochemical deposition, crystal growth, and dielectric breakdown. There has been increasing interest in the physical mechanisms governing the geometrical structure in the diffusion-limited aggregation (DLA). The fractal nature of the aggregate has been analyzed by computational, experimental, and analytical methods. Several analytical attempts, including mean-field theories 12-15 and renormalization-group methods 16-21 have been made to calculate the fractal dimension and the multifractal structure^{22,23} of the growth probability distribution. Several approaches to simple generalizations of the DLA model have been carried out to take into account sticking probability, 1-3 surface tension, 24-26 particle drift, 27-29 multiparticle effects, 3,30 and lifetime effects.³¹ The crossover phenomena from DLA fractal to the nonfractal structure were found by computational and experimental methods. The effect of the sticking probability P on the fractal nature of DLA has been studied by the computer simulation.^{2,3,32} When the diffusive particle reaches a site that is nearest to the aggregate, it now has the probability P of sticking. It has been found that when P is small, the aggregate is apparently more compact for intermediate sizes; above a characteristic size the fractal character emerges. However, one can easily be convinced that in the limit $P \rightarrow 0$ one must recover the Eden model. In this limit, the Brownian particle visits all the surface sites many times before sticking. Then the sticking probability becomes uniform over the whole surface as in the Eden model. Thus an open question concerns the asymptotic behavior of DLA in which the sticking probability P is not one. A similar question is also shown in the viscous fingering at the finite viscosity ratio. Very recently, Lee, Coniglio, and Stanley³³ succeeded in analyzing the crossover from the DLA fractal to the dense structure in viscous fingering at the finite viscosity ratio by using the two-parameter position-space renormalization-group method. The position-space renormalization-group approach for DLA devised by Nagatani¹⁸ was extended to the crossover phenomena.

In this paper, we consider the effect of the sticking probability on the fractal nature of the DLA. The extended version of DLA introducing the sticking probability P is equivalent to the Laplacian growth model with the third boundary condition, since the DLA is isomorphic to the Laplacian growth.³⁴ The third boundary condition on the surface of the aggregate is given by

$$(1-P)\frac{\partial\Phi}{\partial n} - P\Phi = 0 , \qquad (1)$$

where Φ is the scalar potential satisfying the Laplace equation, and $\partial \Phi / \partial n$ the derivative normal to the interface. The limiting case of P=1 represents the ordinary DLA model with the perfectly absorbing boundary. In the limit of $P \rightarrow 0$, it gives the perfectly reflecting boundary and the Eden model is reproduced since the probability visiting the surface becomes uniform over all the surface site. We consider the crossover phenomena from the nonfractal structure to the DLA fractal. By using the two-parameter position-space renormalization-group method, the crossover from the dense structure to the DLA fractal is analyzed. With the sticking probability P < 1, the system crosses eventually over to the DLA fractal.

The organization of the paper is as follows. In Sec. II we present the dielectric breakdown model on the diamond hierarchical lattice for DLA with the sticking probability. In Sec. III we apply the two-parameter position-space renormalization-group method to the dielectric breakdown model. In Sec. IV we present a global flow diagram in two-parameter space. The crossover from the dense structure to the DLA fractal is shown. In Sec. V we present the summary.

II. MODEL

We use an electrostatic analogy to transform the DLA problem into a specific type of resistor network problem. We describe DLA in the dielectric breakdown language. The dielectric breakdown model is isomorphic to the DLA, since both systems are governed by the Laplace equation. For simplicity, we consider the problem on the diamond hierarchical lattice. The position-space renormalization-group approach applied to the hierarchical lattice is comparatively accurate to derive the critical behavior of the system. The diamond hierarchical lattice is constructed by an iterative generation of the base set (Fig. 1). Each bond is occupied by a resistor of unit conductance. A constant voltage is applied between the bottom and the top on the diamond hierarchical lattice. The dielectric breakdown proceeds from the bottom to the top. Figure 2 shows the illustration of the breakdown model on the diamond lattice. The thick lines indicate breakdown bonds: superconducting bonds that construct the breakdown pattern. The bonds on the perimeter of the breakdown pattern are represented by the wavy lines. The thin lines indicate unbroken bonds, which are resistors of unit conductance. So the resistor network problem is solved under a discrete version of the boundary condition (1). On the perimeter bond, the boundary condition is given by

$$(1-P)(\Phi_{ns}-\Phi_{s})-P\Phi_{s}=0$$
, (2)

where Φ_s is the potential of a site on the surface of the aggregate, and Φ_{ns} the potential of a nearest-neighbor site of the aggregate. The potential Φ_s is interpreted as the voltage drop which occurs from the contact resistance between the aggregate and the bulk. A growth probability proportional to the current is then assigned to the perimeter bond. The interface proceeds to the top according to the growth probability. The breakdown process of bonds is assumed to occur one by one. The growth probability p_i at the growing-perimeter bond i is given by

$$p_i \sim I_i$$
 , (3)

where I_i is the local current at the growth bond i. Thus we can describe DLA with the sticking probability in terms of the breakdown model on the resistor network with a contact resistance.

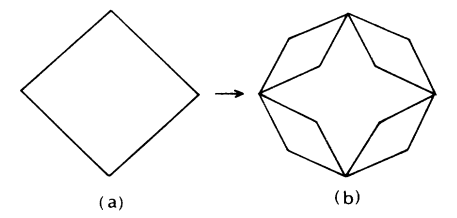


FIG. 1. Generation of the diamond hierarchical lattice. (a) Base set. (b) Second stage.

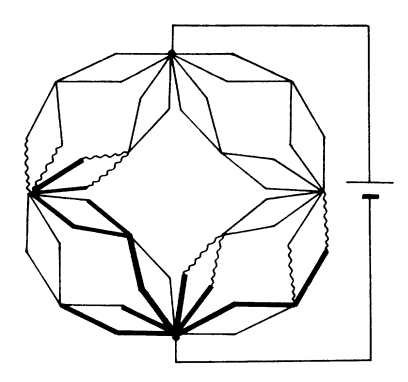


FIG. 2. Illustration of the dielectric breakdown model with the contact resistance. A constant voltage is applied between the bottom and the top. The thick, wavy, and thin lines indicate, respectively, breakdown, growth, and unbroken bonds.

III. RENORMALIZATION-GROUP APPROACH

We consider the renormalization procedure for deriving the two-parameter position-space renormalization-group equations. We derive the renormalization transformations for the sticking probability P and the surface conductance σ_s of the perimeter bond. We will show that the two-parameter renormalization-group equations are given by

$$P' = R_P(P, \sigma_s) , \qquad (4)$$

$$\sigma_s' = R_s(P, \sigma_s) . ag{5}$$

We distinguish between three types of bonds on the lattice before and after a renormalization procedure: (a) interior bonds which are occupied by superconducting bonds and construct the aggregate, (b) growth bonds which are on the surface of the aggregate and can be successively grown, and (c) exterior bonds which construct the electric field in the exterior of the aggregate. The interior, growth, and exterior bonds are, respectively, indicated by the thick, wavy, and thin lines in the figures. We partition all the space of the diamond hierarchical lattice into cells of size b = 2 (b is the scale factor), each containing a single generator. After a renormalization transformation these cells play the role of "renormalized" bonds. The nth generation of the hierarchical lattice is transformed to the (n-1)th generation. The renormalized bonds are then classified into the three types of bonds, similarly to bonds before the renormalization. If the cell is spanned with the bonds occupied by the interior bond, then the cell is renormalized as the interior bond. If the cell is not spanned with the interior bond and is nearest neighbor to the aggregate, then the cell is renormalized as the growth bond on the surface. When the cell is constructed only by the exterior bonds and not nearest neighbor with the aggregate, then the cell is renormalized as the exterior bond. The conductance of the interior bond remains an infinite value after renormalization. The conductance of the exterior bond after renormalization also remains a unit value. The conductance of the renormalized bond as the growth bond is transformed to a different value after renormalization. We call the conductance of the growth bond as the surface conductance. The sticking probability P is transformed to a different value P' after renormalization of the cell to be possible to renormalize as the growth bond on the perimeter.

We assume that DLA process occurs stepwise: the breakdown proceeds one by one, and only one bond breaks at a time (there is no simultaneous bond breaking). We derive the renormalization-group equations for the sticking probability P and the surface conductance σ_s . Figure 3 shows all the configurations of the cell for which it is possible to renormalize as the growth bond. Let us consider the configurational probability \boldsymbol{C}_{α} with which a particular configuration α appears. The distinct configurations are labeled by α ($\alpha = 0, 1, 2$) in Fig.3. The configuration (1) is constructed by adding a breakdown bond onto the growth bonds 1 or 2 in the configuration (0). The probability with which a breakdown bond adds onto the growth bonds 1 or 2 in the configuration (0) is given by the growth probabilities $p_{0,1}$ or $p_{0,2}$ of the growth bonds 1 or 2 in the configuration (0). In addition, by adding a breakdown bond to the configuration (1), the configuration (2) occurs. We here assume that the breakdown proceeds one by one. The configurational probabilities C_{α} are given by

$$C_1 = C_0(p_{0,1} + p_{0,2}), \quad C_2 = C_1 p_{1,2},$$
 (6)

where $p_{0,1} = p_{0,2} = \frac{1}{2}$. The configurational probability C_0 is determined from the normalization condition

$$\sum_{\alpha} C_{\alpha} = C_0 + C_1 + C_2 = 1 . (7)$$

Consider the resistor network problem for cells that can be renormalized as a growth bond pattern. The electric fields within the cell are determined by the surface conductance σ_s and the sticking probability P. We solve the resistor network problem for deriving the renormalization functions (4) and (5) of the sticking probability P and the surface conductance σ_s . We apply the unit voltage between the top and the bottom for each cell (see Figs. 4–6 below). Figure 4 shows the resistor network problem for the configuration (0). The resistor network consisting of the four bonds on the left-hand side is transformed to the single resistor with the equivalent electric property. By using the boundary condition (2), the voltages and the currents within the cell are determined. The total current and the total conductance of the cell are given by

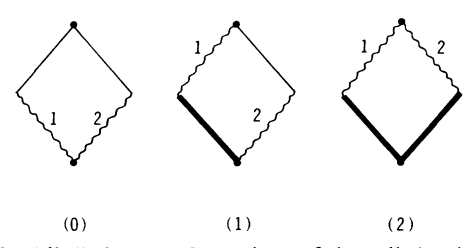


FIG. 3. All distinct configurations of the cell that it is possible to renormalize as the growth bond.

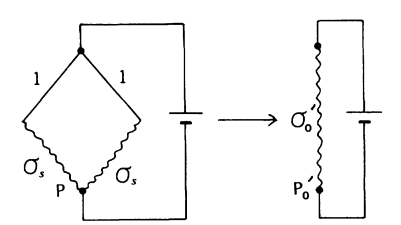


FIG. 4. The resistor network problem for the configuration (0). The circuit on the left-hand side is renormalized to that on the right-hand side. Both circuits are electrically equivalent.

$$I_0 = 2P\sigma_s / (1 + P\sigma_s), \quad \sigma_0' = 2\sigma_s / (1 + \sigma_s).$$
 (8)

The voltage V'_s on the surface of the renormalized bond is determined from

$$(1-P_0')(1-V_s')-P_0'V_s'=0, (9)$$

where P' is the renormalized sticking probability. The total current flowing in the cell equals to the current flowing through the renormalized bond:

$$I_0 = \sigma_0'(1 - V_s') \ . \tag{10}$$

By using Eqs. (8)-(10), the renormalized sticking probability P'_0 is obtained:

$$P_0' = (1 + \sigma_s)P/(1 + P\sigma_s)$$
 (11)

Similarly to the configuration (0), we solve the resistor network problem for the configuration (1) (see Fig. 5). The total current flowing within the cell is given by

$$I_1 = \sigma_s P(2 + \sigma_s P) / (1 + \sigma_s P)$$
 (12)

The total conductance of the cell is given by

$$\sigma_1' = \sigma_s(2 + \sigma_s)/(1 + \sigma_s) . \tag{13}$$

By using the condition that the total current flowing within the cell equals to that carrying through the renormalized bond, the renormalized sticking probability P'_1 is given by

$$P_1' = P(2 + \sigma_s P)(1 + \sigma_s)/(1 + \sigma_s P)(2 + \sigma_s)$$
 (14)

The growth probabilities $p_{1,1}$ and $p_{1,2}$ within the cell are given by

$$p_{1,1} = (1 + \sigma_s P)/(2 + \sigma_s P)$$
,
 $p_{1,2} = 1/(2 + \sigma_s P)$. (15)

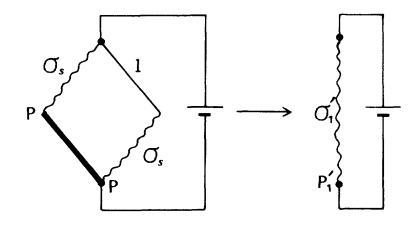


FIG. 5. The resistor network problem for the configuration (1). The circuit on the left-hand side is renormalized to that on the right-hand side.

Similarly, the conductance σ'_2 of the cell with the configuration (2) is obtained:

$$\sigma_2' = 2\sigma_s . \tag{16}$$

Figure 6 shows the resistor network problem for the configuration (2). The renormalized sticking probability P'_{2} of the cell is given by

$$P_2' = P . (17)$$

The growth probabilities $p_{2,1}$ and $p_{2,2}$ are given by

$$p_{2,1} = \frac{1}{2}, \quad p_{2,2} = \frac{1}{2}$$
 (18)

When the sticking probability P equals to one, the conductances $\sigma_{\alpha'}$ and the growth probabilities $p_{\alpha,i}$ are consistent with those of the ordinary DLA. The renormalized conductance σ'_s of the growth bond will be assumed to be given by the most probable value

$$\sigma_s' = \exp\left[\sum_{\alpha} C_{\alpha} \ln \sigma_{\alpha}'\right]. \tag{19}$$

The relationship (19) with (8), (13), and (16) presents the renormalization-group equation $\sigma'_s = R_s(P, \sigma_s)$ for the surface conductance. The renormalized sticking probability P' will be assumed to be given by the mean value

$$P' = \sum_{\alpha} C_{\alpha} P'_{\alpha} \ . \tag{20}$$

The relationship (20) with (11), (14), and (17) presents the renormalization-group equation $P' = R_P(P, \sigma_s)$ for the sticking probability. Equations (6)-(8), (11), (13)-(20)are simultaneously solved. We find the two nontrivial fixed points $(0, \sigma_E^*)$ and $(1, \sigma_{DLA}^*)$ where $\sigma_E^* = 2.611$ and $\sigma_{\mathrm{DLA}}^*=2.123$, respectively. At the fixed point $(0,\sigma_E^*)$, the growth probabilities $p_{\alpha,i}$ give $\frac{1}{2}$ for all the growth bonds in the configurations (0), (1), and (2). The growth probability on the growth bonds over the whole system is represented by the multiplicative process of the cell's growth probabilities. 18 The growth probability over the whole system becomes uniform over all the surface bond. The fixed point $(0, \sigma_E^*)$ corresponds to the Eden model. It is called the Eden point. On the other hand, the fixed point $(1, \sigma_{DLA}^*)$ gives the ordinary DLA. It is called the DLA point. In the following section, we study the stability of the fixed points in the two-parameter space (P, σ_s) . The global flow in the two-parameter space (P, σ_s) will be obtained. The crossover phenomena are investigated.

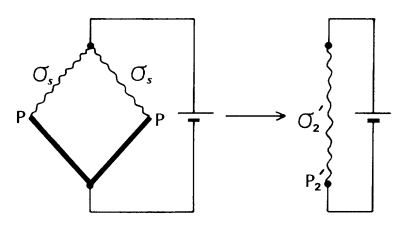


FIG. 6. The resistor network problem for the configuration (2). The circuit on the left-hand side is renormalized to that on the right-hand side.

IV. CROSSOVER FROM NONFRACTAL TO DLA FRACTAL

We consider the crossover phenomena from the Eden model to the DLA fractal. To find the global flow diagram in the two-parameter space (P, σ_s) , we randomly choose a point in the parameter space (P, σ_s) , and calculate the renormalized sticking probability and the renormalized surface conductance using (19) and (20), to find a new point (P', σ'_s) . We repeat this process to find next point (P'', σ_s'') , and continue until we approach a stable fixed point. We use 50 initial points and plot the renormalization flow in the phase space for representative initial points. Figure 7 shows the renormalization flow, obtained by using (19) and (20). From the renormalization flow, we can determine the stabilities of the two fixed points: the Eden and the DLA points. The Eden point is a saddle point: it is stable in the y direction, and unstable in other directions. The DLA point is stable in every direction. All the renormalization flows eventually merge into the DLA point. It is found from the flow diagram that there exists a crossover from the dense cluster (the Eden fixed point) to the DLA fractal (the DLA fixed point). The crossover line can be determined by following the renormalization flow which starts from an initial point very close to the Eden fixed point. It is indicated by the thick line in Fig. 7. In order to quantify this crossover behavior, we define a crossover exponent ϕ and a crossover radius r_{\times} . We propose the scaling ansatz along the crossover line,

$$M(r,P) = r^d F(Pr^{\phi}) , \qquad (21a)$$

where M is the mass of the cluster, r the radius of gyration, d the embedding dimension, and P the sticking probability. The similar scaling form was already proposed by Meakin.³⁵ We assume

$$F(x) \sim \begin{cases} 1 & \text{if } x \ll 1, \\ x^{\alpha} & \text{if } x \gg 1. \end{cases}$$
 (21b)

As r increases, M(r,P) scales as $r^{d+\phi\alpha}$. With increase of r, the aggregate becomes DLA fractal, implying

$$d + \phi \alpha = d_f \tag{22}$$

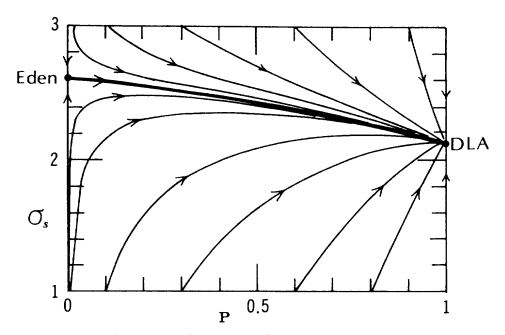


FIG. 7. Global flow diagram in two-parameter space (P, σ_s) . There are two fixed points: the Eden and the DLA points. All the renormalization flows eventually merge into the DLA point. The crossover line from the Eden to the DLA is indicated by the thick line.

where d_f is the fractal dimension of DLA. Furthermore, we can estimate r_{\times} . From (21b), r_{\times} should be the value of the radius which corresponds to x=1, that is $r_{\times} \sim P^{-1/\phi}$. The crossover exponent ϕ shall be found by linearizing the renormalization equations and calculating the eigenvalues. The linearized relation of the renormalization equations is given by

$$\begin{bmatrix} \delta P' \\ \delta \sigma'_{s} \end{bmatrix} = \begin{bmatrix} \frac{\partial R_{P}}{\partial P} & \frac{\partial R_{P}}{\partial \sigma_{s}} \\ \frac{\partial R_{s}}{\partial P} & \frac{\partial R_{s}}{\partial \sigma_{s}} \end{bmatrix}_{\text{Edgn}} \begin{bmatrix} \delta P \\ \delta \sigma_{s} \end{bmatrix}, \tag{23}$$

where the matrix is evaluated at the Eden fixed point. The values of the matrix elements are numerically calculated from the renormalization functions. The eigenvalues of the matrix are obtained

$$\lambda_1 = 2.27$$
 and $\lambda_2 = 0.649$. (24)

The crossover exponent ϕ is given by

$$\phi = \ln \lambda_1 / \ln b = 1.18 . \tag{25}$$

Meakin³⁵ found the following scaling form from the computer simulation

$$M(r,P) = r^{2.11} f(Pr^{0.88})$$
 (26)

This should be compared to the result (21a) with (25). Consequently, the theoretical result and the computer simulation result appear to be consistent with each other.

There are already some simulations^{23,32,35} indicating that the crossover from the dense structure to the DLA fractal shown by our approach may be correct; e.g., the simulated patterns are thicker near the starting point

than near the periphery and above a characteristic radius the fractal structure shows up. The comparison of this crossover with that in the viscous fingering is very interesting. By using the position-space renormalization-group method, Lee, Coniglio, and Stanley³³ found that in viscous fingering at a finite viscosity ratio, the crossover occurred from the DLA fractal to the compact cluster. The crossover from the DLA fractal to the compact cluster is in contrast to that found above: the crossover from the dense structure to the DLA fractal.

V. SUMMARY

We propose a Laplacian growth model with the third boundary condition (a linear combination of Dirichlet and Neumann boundary conditions) to study the effect of the sticking probability on the diffusion-limited aggregation. We develop a set of the position-space renormalization-group equations for DLA with the sticking probability. By using the two-parameter position space renormalization-group method, we find that the crossover occurs from the dense structure to the DLA fractal when the sticking probability is small. The two nontrivial fixed points: the Eden point and the DLA point are found. It is found that when the sticking probability is less than one, the aggregate crosses eventually over to the DLA fractal. We calculate the crossover exponent and the crossover radius.

ACKNOWLEDGMENTS

The author would like to thank Professor H. E. Stanley for informing him of related works. Dr. Lee is also acknowledged for his sending the author papers before publication.

¹T. A. Witten and L. M. Sander, Phys. Rev. Lett. 47, 1400 (1981); Phys. Rev. B 27, 5686 (1983).

²P. Meakin, Phys. Rev. A **26**, 1495 (1983); **27**, 604 (1983); **27**, 2616 (1983).

³R. F. Voss, J. Stat. Phys. **36**, 861 (1984).

⁴Kinetics of Aggregation and Gelation, edited by F. Family and D. P. Landau (North-Holland, Amsterdam, 1984).

⁵On Growth and Form, edited by H. E. Stanley and N. Ostrowsky (Nijhoff, The Hague, 1985).

⁶Fractals in Physics, edited by L. Pietronero and E. Tosatti (North-Holland, Amsterdam, 1986).

⁷P. Meakin, in *Phase Transition and Critical Phenomena*, edited by C. Domb and J. L. Lebwitz (Academic, New York, 1988), Vol. 12, p. 336.

⁸R. Julien and R. Botet, Aggregation and Fractal Aggregates (World Scientific, Singapore, 1987).

⁹J. Feder, Fractals (Plenum, New York, 1988).

¹⁰Random Fluctuations and Pattern Growth, edited by H. E. Stanley and N. Ostrowsky (Kluwer Academic, Dordrecht, 1988)

¹¹T. Vicsek, Fractal Growth Phenomena (World Scientific, Singapore, 1989).

¹²M. Muthukumar, Phys. Rev. Lett. **50**, 839 (1983).

¹³M. Tokuyama and K. Kawasaki, Phys. Lett. **100A**, 337 (1984).

¹⁴R. C. Ball, Physica A **140**, 62 (1986).

¹⁵K. Honda, H. Toyoki, and M. Matsushita, J. Phys. Soc. Jpn. 55, 707 (1986).

¹⁶H. Gould, F. Family, and H. E. Stanley, Phys. Rev. Lett. **50**, 686 (1983).

¹⁷N. Nakanishi and F. Family, Phys. Rev. A **32**, 3606 (1985).

¹⁸T. Nagatani, J. Phys. A 20, L381 (1987); Phys. Rev. A 36, 5812 (1987); 38, 2632 (1988); J. Phys. A 21, L655 (1988).

¹⁹L. Pietronero, A. Erzan, and C. Evertsz, Phys. Rev. Lett. **61**, 861 (1988).

²⁰J. Lee, P. Alstrom, and H. E. Stanley, Phys. Rev. A 39, 6545 (1989).

²¹X. R. Wang, Y. Shapir, and M. Rubinstein, Phys. Rev. A 39, 5974 (1989); J. Phys. A 22, L507 (1989).

²²T. C. Halsey, P. Meakin, and I. Procaccia, Phys. Rev. Lett. **56**, 854 (1986).

²³C. Amitrano, A. Coniglio, and F. di Liberto, Phys. Rev. Lett. 57, 1016 (1986).

²⁴T. Vicsek, Phys. Rev. A 32, 3084 (1985).

- ²⁵L. P. Kadanoff, J. Stat. Phys. **39**, 267 (1985).
- ²⁶R. Tao, M. A. Novotny, and K. Kashi, Phys. Rev. A 38, 1019 (1988).
- ²⁷P. Meakin, Phys. Rev. B 28, 5221 (1983).
- ²⁸R. Kapral, S. G. Whittington, and R. C. Desai, J. Phys. A 19, 1727 (1986).
- ²⁹T. Nagatani, Phys. Rev. A **39**, 438 (1989).
- ³⁰M. Uwaha and Y. Saito, J. Phys. Soc. Jpn. **57**, 3285 (1988).
- ³¹S. Miyajima, Y. Hasegawa, A. Bunde, and H. E. Stanley, J. Phys. Soc. Jpn. **57**, 3376 (1988).
- ³²Julien and Botet, Aggregation and Fractal Aggregates (Ref. 8), p. 65.
- ³³J. Lee, A. Coniglio, and H. E. Stanley (unpublished).
- ³⁴L. Pietronero and H. J. Wiesmann, J. Stat. Phys. **36**, 909 (1984).
- ³⁵P. Meakin, Ann. Rev. Phys. Chem. **39**, 237 (1988).